Materials Letters 185 (2016) 573–575

Contents lists available at ScienceDirect

Materials Letters

journal homepage: www.elsevier.com/locate/matlet

Performance improvement of temperature sensor based on rare-earth ion fluorescence by using KBr-diluted phosphor

Ning Yuan[a,1], Hong-Xue Sun[a,1], Zi-Bo Zhang[b], Qi Sun[a], Wing-Han Wong[a,c], Dao-Yin Yu[a], Edwin Yue-Bun Pun[c], De-Long Zhang[a,c,*]

[a] School of Precision Instruments and Opto-electronics Engineering, Tianjin University, Tianjin 300072, China
[b] Faculty of Engineering, University of Toulouse 3, F-31062 Toulouse, France
[c] Department of Electronic Engineering and State Key Laboratory of Millimeter Waves, City University of Hong Kong, Kowloon, Hong Kong, China

ARTICLE INFO

Keywords:
Optical temperature sensor
Fluorescence intensity ratio (FIR)
KBr dilution
Sensing performance

ABSTRACT

We exemplify the $Er(NbO_3)_3$ phosphor to demonstrate that the performance of the temperature sensor based on thermal effect of fluorescence intensity ratio (FIR) of 980-nm-upconverted Er^{3+} green 530 and 550 nm emissions can be improved by using KBr-diluted phosphor. The sensing performance of the diluted phosphor plate was studied as a function of KBr:$Er(NbO_3)_3$ molar ratio from 0:1 to 100:1. The results show that the KBr dilution enables to enhance the fluorescence intensity and increase the temperature sensitivity. Meanwhile, the KBr itself does not affect either the Er^{3+} spectroscopic properties or the FIR value. There is an optimum KBr:$Er(NbO_3)_3$ molar ratio within 15:1 and 20:1, for which the 530 (550) nm signal increases by 30% (20%) and the relative sensitivity at the physiological temperature increases by 14%.

1. Introduction

Optical temperature sensing based on fluorescence intensity ratio (FIR) continues to draw attention [1–8]. The method is based on the comparison of the fluorescence intensities of two emissions from two closely spaced energy levels to a lower state of rare-earth ion. The two green emissions $^4S_{3/2}\rightarrow{}^4I_{15/2}$ (550 nm) and $^2H_{11/2}\rightarrow{}^4I_{15/2}$ (530 nm) of Er^{3+} are particularly suitable for this application. A practical sensor is required to have good signal-to-noise ratio and high sensitivity. Here, we exemplify the $Er(NbO_3)_3$ phosphor to demonstrate that the performance of the temperature sensor based on the FIR of Er^{3+} green 530 and 550 nm emissions can be improved by using KBr-diluted phosphor. The idea is motivated by the well-known KBr-pellet technique, which is usually used to measure the optical absorption of unclear phosphor powder.

2. Experiment

The $Er(NbO_3)_3$ phosphor was prepared by sintering a homogeneous mixture of (Er_2O_3+3Nb_2O_5) at 1200 °C for 76 h. The crystalline phase in the mixture was analyzed by a Siemens D500 diffractometer. The grain size was analyzed by a Malvern 2000 laser particle size analyzer. The upconversion emission spectra were recorded by a SPEX 500M monochromator under the excitation of 975 nm/50 mW.

The $Er(NbO_3)_3$ phosphor was homogeneously mixed with KBr according to different KBr:$Er(NbO_3)_3$ molar ratios R ranging from 0:1 to 100:1. Table 1 shows the R value for each sample. Each mixture was pressurized into a 1 mm thick plate.

Fig. 1 shows the structural schematic of the sensor. The 980 nm/50 mW excitation light is incident onto the phosphor. After collimated by a lens (L_1), the fluorescence was focused by another lens (L_2) and detected by a Si-photocell. A 530 or 550 nm interference filter was placed in front of the photocell. The 530 or 550 nm photovoltaic signal was detected by a multimeter. The sample was heated via the thermo-electrically ceramic plate. The temperature was measured by an infrared thermometer with an accuracy ± 0.5 °C.

3. Results and discussion

As the powder diffraction file of the $Er(NbO_3)_3$ could not be found in the literatures, the new phase formed in the calcined Er_2O_3+3Nb_2O_5 mixture is justified by comparing its x-ray diffraction pattern with those patterns of the raw materials Er_2O_3 and Nb_2O_5 and other possibly formed phases, $ErNbO_4$ [9] and Er_3NbO_7 [10], which are shown in Fig. 2. Comparison shows that a new phase $Er(NbO_3)_3$ is formed. The size of the $Er(NbO_3)_3$ grains is 2–11 μm as shown in the inset in Fig. 2.

* Corresponding author at: School of Precision Instruments and Opto-electronics Engineering, Tianjin University, Tianjin 300072, China.
E-mail address: dlzhang@tju.edu.cn (D.-L. Zhang).
[1] Equally contributed authors.

http://dx.doi.org/10.1016/j.matlet.2016.09.081
Received 23 June 2016; Received in revised form 1 September 2016; Accepted 20 September 2016
Available online 21 September 2016
0167-577X/

Table 1
FIR parameters and S value at 310 K for different R values.

R	B	$\Delta E/k_B$ (K)	S @310 K ($\times 10^{-3}$ K^{-1})
0:1	9.0	685.0	7.0
5:1	12.7	729.6	7.6
10:1	8.0	741.5	7.7
15:1	10.0	761.0	8.0
20:1	6.5	702.1	6.8
30:1	9.3	741.5	7.3
50:1	3.3	519.1	5.4
100:1	5.7	585.7	6.1

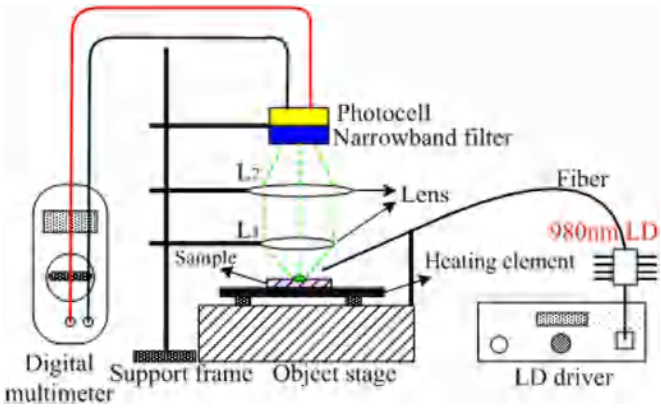

Fig. 1. Structural schematic of the temperature sensor.

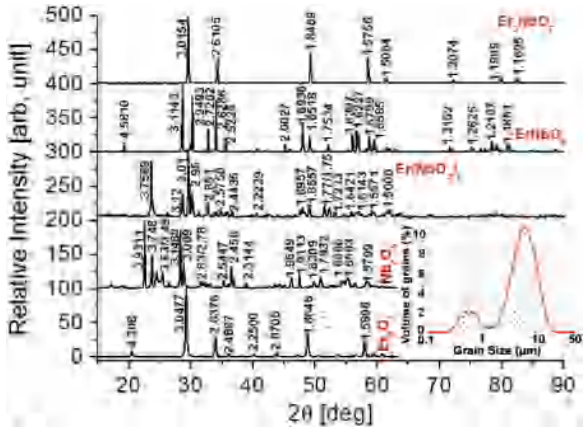

Fig. 2. X-ray diffraction patterns of $Er(NbO_3)_3$, Er_2O_3, Nb_2O_5, $ErNbO_4$ and Er_3NbO_7. The inset shows the size distribution of the $Er(NbO_3)_3$ grains.

A comparison of the fluorescent spectra of the KBr-diluted (R=15:1) and undiluted phosphors shows that KBr dilution affects little the spectral shape but causes fluorescence enhancement, which is verified by the photocell response. Fig. 3 shows the photocell response to the 550 and 530 nm fluorescence measured at 296 K. The response is plotted against the R value. It is evident that the fluorescence intensity shows definite dilution effect. The general trend is non-monotonous and similar for both the 550 nm and 530 nm fluorescence. For the sample without KBr dilution, because of its opaque feature the excitation only takes place at its near surface, resulting in fewer active ions being excited and hence weak fluorescence. In the dilution case, the sample transparency increases with the KBr content, the pump light penetrates deeper, more Er^{3+} ions are excited, though Er^{3+} concentration lowers in some extent due to the dilution. As a result, the photocell response increases with a rise in KBr content. For the highly diluted phosphor, the Er^{3+} concentration lowers largely, the fluorescence intensity and hence the output drops. It is thus comprehensible that a maximum output is obtained for R=20:1, for which the

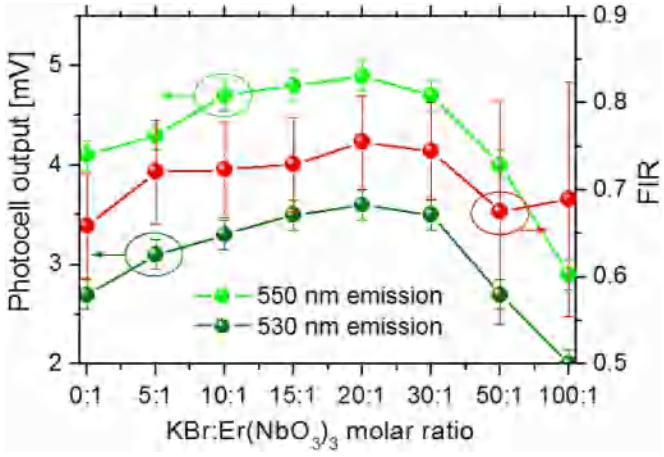

Fig. 3. Photocell response to the 550 nm (green balls) and 530 nm (olive balls) fluorescence measured at 296 K, and the corresponding FIR value versus R value. (For interpretation of the references to color in this figure legend, the reader is referred to the web version of this article.)

530 (550) nm output increases by 30% (20%).

Based on Fig. 3 we have calculated the FIR against the R value [$FIR=I_H/I_S$ with I_H (I_S) denoting the 530 (550) nm fluorescence intensity]. The results are shown in Fig. 3 too. We note that the FIR can be thought as unchanged within the error, implying that the KBr itself does not affect the FIR value.

Next, attention is paid to the sensing characteristics of the KBr-diluted phosphor. Fig. 4 shows the temperature dependence of photocell output in the temperature range 296–403 K for the 550 nm (a) and 530 nm (b) fluorescence of the samples with different R values. We note that the photocell output decreases with a rise in temperature because of thermal quench effect. The 550 nm emission decreases more significantly because of thermalized effect between $^2H_{11/2}$ and $^4S_{3/2}$ [11,12]. In addition, the dilution effect on the fluorescence intensity is still evident for T > 296 K.

From Fig. 4 we have calculated at first the ln(FIR) against 1/T for each sample, and then done a linear fit. By correlating each fitting expression with $FIR=I_H/I_S=Bexp[-\Delta E/(k_BT)]$, we obtain the pre-exponential factor B and energy gap ΔE or $\Delta E/k_B$. The results are summarized in Table 1. With the known ΔE value, we can calculate the relative sensitivity $S=(1/FIR)d(FIR)/dT=(\Delta E/k_B)/T^2$ as a function of the temperature for each R value, named S-R plot. Calculation shows that, except for the two S-R plots with the large R values 50:1 and 100:1, which cause poor signal-to-noise ratio due to too low Er^{3+} concentration, all of the other plots of the KBr-diluted samples are located above the one of the undiluted sample, implying that the dilution induces the increase of S. Aiming at the biological application, the S values at the physiological temperature 310 K are summarized in Table 1. One can see that there is an optimum R value around 15:1, for which the S value at the 310 K, 8×10^{-3} K^{-1}, is promoted by 14% relative to the value of undiluted sample, ~7×10^{-3} K^{-1}.

It appears from Table 1 that $\Delta E/k_B$ changes slightly with R value as R≤ 30 while decreases abruptly as R > 30. In principle, the dilution should not affect the electronic energy structure of Er^{3+}. We assume the abrupt decrease of ΔE for R > 30 is related to too poor signal-to-noise ratio due to too low Er^{3+} concentration, and the $\Delta E/k_B$ values for R=50 and 100 are not reliable that are given as a reference only. As for the slight dilution effect on ΔE for R < 30, it is also not really that dilution affects the ΔE, but is associated with phonon energy effect on the multi-phonon non-radiative rate. The lower phonon energy of KBr host (< 250 cm^{-1} [13]) affects the S value via its effect on the multi-phonon non-radiative rate [12]. The effect is equivalent to the relative increase of ΔE. In addition, the KBr absorption upon the pump light (the KBr absorption coefficient at the 0.98 μm wavelength is ~10 cm^{-1}) aids to

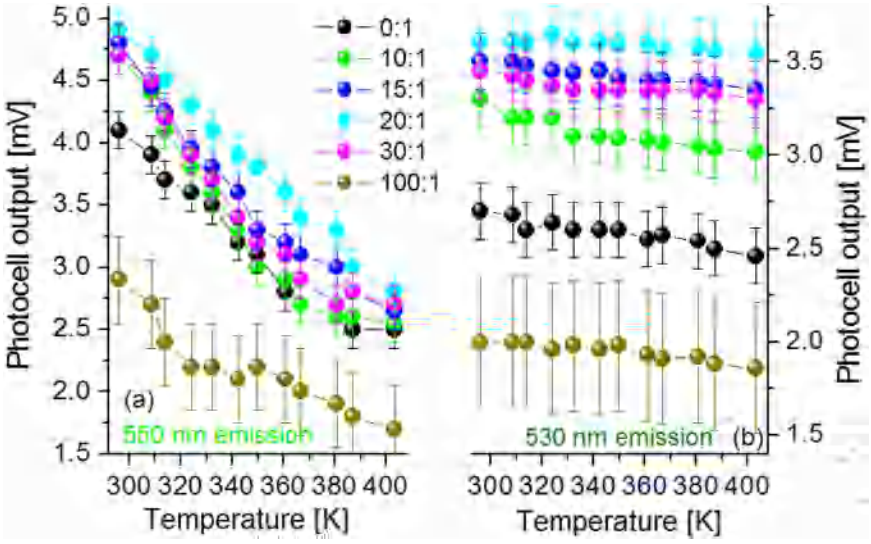

Fig. 4. Temperature dependence of photocell output for (a) 550 nm and (b) 530 nm fluorescence of the sample plates with different R values.

heat the phosphor. The effect is equivalent to the relative ΔE increase too.

The phosphor thermometry is commonly applied to the surface, gas phase and liquid. This requires the sensing film is thin and the phosphor grain size is small as soon as possible. Regarding the present method, if the dilution is only effective for the thick plates (> 50 μm), the practical use of the method will be limited in many situations. Our additional experiments have shown that the dilution is effective for the plate thickness down to 40 μm. By employing an adequate pellet setup, an even thinner film could be obtained, predicting the application potential of the method.

4. Conclusions

We exemplify micro-sized $Er(NbO_3)_3$ phosphor to demonstrate that the KBr dilution enables to improve sensing performance, meanwhile, the KBr itself does not affect either the Er^{3+} spectroscopic characteristics or the FIR value. There is an optimum R value within 15:1 and 20:1, for which the 530 (550) nm signal output increases by 30% (20%) and the sensitivity at 310 K is promoted by 14%. The KBr-dilution scheme can be presumably applied to other glassy or crystalline powder or ceramic phosphors doped with various rare-earth ions.

Acknowledgements

This work was supported by National Natural Science Foundation of China under Project nos. 50872089, 61077039, 61377060 and 61628501, by Research Grants Council of the Hong Kong Special Administrative Region, China, under Project no. 11211014, by Tianjin Science and Technology Commission of China under Project no.16JCZDJC37400.

Appendix A. Supporting information

Supplementary data associated with this article can be found in the online version at doi:10.1016/j.matlet.2016.09.081.

References

[1] K. Soni, et al., Sens. Actuators B: Chem. 216 (2015) 64–71.
[2] A. Wickberg, et al., Appl. Phys. Lett. 106 (2015) 133103.
[3] M.K. Mahata, et al., Sens. Actuators A: Phys. 209 (2015) 775–780.
[4] H. Zou, et al., AIP Adv. 4 (2014) 127157.
[5] P. Du, et al., Appl. Phys. Lett. 104 (2014) 152902.
[6] X.D. Wang, et al., Chem. Soc. Rev. 42 (2013) 7834–7869.
[7] M. Quintanilla, et al., Appl. Phys. Exp. 4 (2011) 022601.
[8] L. Marciniak, et al., J. Phys. Chem. C 120 (2016) 8877–8882.
[9] D.L. Zhang, E.Y.B. Pun, J. Alloy. Compd. 370 (2004) 315–320.
[10] D.L. Zhang, et al., J. Lumin. 127 (2007) 453–460.
[11] L. Núñez, et al., Appl. Phys. B 62 (1996) 485–491.
[12] L.A. Riseberg, H.W. Moos, Phys. Rev. 174 (1968) 429–438.
[13] E. Burstein, et al., Phys. Rev. 139 (1965) A1239–A1245.